Available online at www.sciencedirect.com
ScienceDirect
Ceramics International 34 (2008) 337–343
CERAMICS INTERNATIONAL
www.elsevier.com/locate/ceramint

Boehmite coating on θ-Al_2O_3 particles via a sol–gel route

Lung-Teng Cheng [a], Mong-Yen Tsai [a], Wenjea J. Tseng [*], Hsing-I. Hsiang [b], Fu-Su Yen [b]

[a] *Department of Materials Engineering, National Chung Hsing University, 250 Kuo Kuang Rd., Taichung 402, Taiwan*
[b] *Department of Resources Engineering, National Cheng Kung University, No. 1 University Rd., Tainan 701, Taiwan*

Received 27 April 2006; received in revised form 24 September 2006; accepted 6 October 2006
Available online 13 December 2006

Abstract

θ-Al_2O_3 powders in slurry form were coated by boehmite nanoparticles prepared from alumina sol that consists of aluminum tri-*sec*-butoxide ($Al(OC_4H_9)_3$) as a precursor. The θ-Al_2O_3 powders presented an iso-electrical point (IEP) at pH ~ 9.2, and formed stable suspensions without notable gravity settling at acidic conditions (pH 3–4). Boehmite nanoparticles with a mean particle size ca. 68 nm were derived from the hydrolysis of $Al(OC_4H_9)_3$ sol. Well-dispersed boehmite/θ-Al_2O_3 aqueous mixtures consisting of 3 and 9 wt.% of boehmite were then prepared by addition of θ-Al_2O_3 powder into the $Al(OC_4H_9)_3$ sol followed then by vigorous agitation at 90 °C and in a pH range 3–4. IR and particle-size measurement both revealed possible coating of boehmite on the θ-Al_2O_3 particles. From TEM observation, "thickness" of the boehmite layer did not vary much with the boehmite concentration. Agglomeration of the particles became nonetheless apparent as the boehmite concentration was increased. The boehmite coating on θ-Al_2O_3 surface inhibited grain growth during the θ- to α-phase transformation upon heating. Mean grain size of the boehmite-coated alumina was substantially smaller than that of the un-coated one.

Keywords: Boehmite; Alumina; Coating; Zeta potential

1. Introduction

Yen and co-workers [1,2] have found θ- to α-phase transformation of Al_2O_3 occurs when θ-Al_2O_3 crystallite exceeds a critical size $d_{c,\theta} = \sim 20–25$ nm (determined from the Scherrer equation on $(2 0 \bar{2})_\theta$) upon heating to a temperature above 1000–1150 °C. A subsequent formation of *one* α-Al_2O_3 nucleus proceeds from the evolution of *one* θ-Al_2O_3 crystallite, and the α-Al_2O_3 nucleus presents a critical crystallite size $d_{c,\alpha} = \sim 17$ nm (determined from the Scherer equation on $(0\ 1\ 2)_\alpha$). Upon continuous heating, growth of the α-Al_2O_3 followed the nucleation by coalescing several α-Al_2O_3 crystallites into one grain with a primary crystallite size d_p typically ~45 nm. The primary α-Al_2O_3 crystallites are energetically favorable to aggregate into clustered colonies, each of which is composed of plural vermicular segments with different orientations [3]. This aggregation together with the finger growth induced by heating [4] tends to increase the physical size of α-Al_2O_3 greater than 100 nm and to make the particle more spherical so that the surface area is reduced.

To prepare ultrafine α-Al_2O_3 particles (typically <100 nm), an attainment of spatially discrete θ-Al_2O_3 powders in given matrix appears critically important in order to avoid an excessive grain growth and the particulate aggregation accompanying the θ- to α-phase transformation upon heating. In this regard, Han et al. [5] prepared submicrometer α-Al_2O_3 from surface-modified γ-Al_2O_3 powders via a sol–gel route, and disclosed that the alumina sol appeared to coat on the surface of γ-Al_2O_3 and acted simultaneously as a dispersant in the process. Yang and Troczynski [6] further compared the dispersion of Al_2O_3 powders in water and alumina sol, respectively. They found that the average agglomerate size of Al_2O_3 in the alumina sol decreased by more than 50% when compared to that in water. Ananthakumar et al. [7] reported that boehmite sol is not only a dispersant for the chemical preparation of Al_2O_3 particles, but also acts as a sintering aid that promotes densification of Al_2O_3 and results in a fine, sintered grain size. Shih et al. [8] coated boehmite on surface of Si_3N_4 powders by dissolving aluminum *sec*-butoxide in acid solution before heating the coated powders to 90 °C. They found that the dispersion, rheology, green density and sintered

---

[*] Corresponding author. Fax: +886 4 2285 7017.
E-mail address: wenjea@dragon.nchu.edu.tw (W.J. Tseng).

0272-8842/$34.00 © 2006 Elsevier Ltd and Techna Group S.r.l. All rights reserved.
doi:10.1016/j.ceramint.2006.10.005

properties were all improved, and they ascribed the improved flow and densification properties to the breakdown of the gelled network in Si_3N_4 suspensions, hence facilitating the boehmite coating on SiC in acids [9]. Coating thickness of the boehmite on SiC was found to increase with the increasing boehmite concentration, when the boehmite weight relative to that of the SiC was kept under 10 wt.%; beyond which, the coating thickness appeared to saturate [10]. In this study, aluminum tri-*sec*-butoxide ($Al(OC_4H_9)_3$) was used as a precursor to prepare aqueous boehmite sol for the coating on θ-Al_2O_3 powders surface at different pH values. The objective is two-fold. First, the dispersion of θ-Al_2O_3 powders in aqueous liquid may be improved so that densely packed, boehmite-coated θ-Al_2O_3 powder compacts may be attainable. Second, the boehmite coating may act as a physical barrier to impede the aggregation of α-Al_2O_3 crystallites into substantially larger grain size during the θ- to α-phase transformation upon heating. Formation of fine-grained, densified α-Al_2O_3 at a reduced sintering temperature may become possible [11].

2. Experimental procedure

2.1. Preparation of boehmite sol

De-ionized water (18 MΩ cm) of 300 ml was titrated with hydrochloric acid (HCl, Riedel-de Haen, Germany) to form pH 4 solution before addition of reagent-grade $Al(OC_4H_9)_3$ of 21.14 g (Aldrich, Germany). An ultrasonication operated at 3 W was applied to the mix by a high frequency homogenizer (Sonicator 3000, Misonix, U.S.A.). The powdered slurry was then vigorously agitated by a magnetic stirrer at 90 °C for 0.5 h and its pH was maintained at pH 4 by additional HCl solution [9,12]. A minute amount of the suspension was centrifuged at a rotational speed of 10,000 rpm for 10 min. The clear supernatant after the centrifugal separation was carefully siphoned out by a glass pipette before being mixed with a minor amount of the original slurry to form uniform dispersions by an ultrasonic agitation (12 W) for zeta potential and particle-size measurement via a dynamic light-scattering analyzer (Zetasizer NS, Malvern Instruments, U.K.). The particle morphology was examined by transmission electron microscopy (TEM, Zeiss EM902A, Germany). The residual sediment after the centrifugal operation was rinsed with de-ionized water for three times, oven-dried at 60 °C and was then lightly ground by mortar and pestle for the X-ray diffractometry (XRD, MAC MXTIII, Japan).

2.2. Aqueous dispersion of θ-Al_2O_3 powders

A commercially available θ-Al_2O_3 powder (Forever Chemical, Taiwan) was used in the study. The powder was mixed with de-ionized water to form slurries with a dilute solids concentration (0.05 wt.%) for the determination of zeta potential and particle size. The suspension pH was adjusted with HCl and NH_4OH (Riedel-de Haen, Germany). Some suspensions were then dropped on silicon wafer and dried for field-emission scanning electron microscopy (FE-SEM, JSM-6700F, JEOL, Japan).

2.3. Preparation of boehmite-coated θ-Al_2O_3 particles

Two hundred and forty five milliliters of de-ioned water with a pre-adjusted pH 3–4 were mixed with 5 g of θ-Al_2O_3 powders, and the slurries were titrated with HCl solution to the original pH value (pH 3–4). $Al(OC_4H_9)_3$ precursors of 0.6538 and 2.0907 g were added therein for the preparation of boehmite/θ-Al_2O_3 mixtures with 3 and 9 wt.% of the boehmite concentration, respectively. The boehmite concentration is the calculated weight of boehmite from the $Al(OC_4H_9)_3$ precursor divided by the total weight of the solids in suspensions. Some of the suspensions were dried in oven at 100 °C. The dried powders were then calcined at 600 °C for 2 h in air atmosphere. The calcined granules were lightly ground, ultrasonically washed with de-ionized water for three times, and injected into an IR card (3M, U.S.A.) for FTIR analysis (Fourier transform infrared spectrometer, RX-I, Perkin-Elmer, U.S.A.) in wavenumbers ranging from 1500 to 400 cm^{-1}.

2.4. Microstructure of sintered boehmite-coated and un-coated Al_2O_3

The un-coated θ-Al_2O_3 powders and the boehmite/θ-Al_2O_3 powders were lightly ground by mortar and pestle, and were pelletized into discs by uniaxial pressing followed then by cold-isostatic pressing at 27 MPa. The green pellets were then sintered in air at 1500 °C with an isothermal holding of 2 h. Fractured surface of the sintered samples was observed by FE-SEM.

3. Results and discussion

3.1. Dispersion of θ-Al_2O_3 suspensions at different pH values

Fig. 1 shows zeta potential and mean particle size of the dilute θ-Al_2O_3 suspensions at different pH values. The zeta

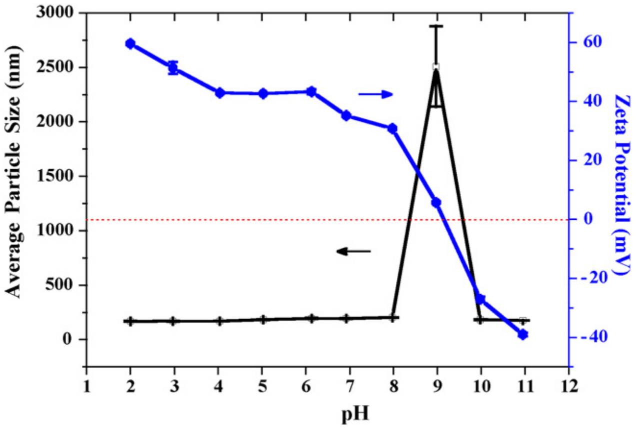

Fig. 1. The mean particle size and zeta potential of dilute θ-Al_2O_3 suspension (solids content 0.05 wt.%) at different pH values.

potential appears to decrease from 60 to 30 mV as the pH increases from 2 to 8, while the mean particle size remains at about 170 nm. A separate sedimentation experiment of the suspensions was conducted. No discernable settlement of the θ-Al_2O_3 was observed after 1 week, revealing a stable suspension. The θ-Al_2O_3 powders present an iso-electrical point (IEP) at pH ~ 9.2. At the IEP, the particles aggregate and form particulate clusters with a pronounced increase in the measured ''particle'' size (~2.5 μm), due presumably to the interparticle van der Waals attraction when the particles were brought together by Brownian motion [13]. When the suspension pH was further increased, i.e., pH ≥ 10, the magnitude of zeta potential increased above 30 mV and the mean particle size of θ-Al_2O_3 powders quickly returned to a level (~180 nm) similar to that of the pH ≤ 8. This indicates that an increased interparticle repulsion arising from the development of electrical double layer results so that the θ-Al_2O_3 dispersion was facilitated. A typical morphology of the dried θ-Al_2O_3 powders at pH 3 is shown in Fig. 2(a); to which, primary θ-Al_2O_3 particles with a size less than 100 nm co-exist with scattered aggregates of submicrometer size. In contrast, Fig. 2(b) is an SEM micrograph of the dried θ-Al_2O_3 powders prepared at pH 9. Particle aggregation is apparent, suggesting a formation of continuous particulate network in the suspension structure. These SEM findings not only vindicate the zeta and particle-size results measured by the light-scattering technique, but also reveal the importance of interparticle potential to the dispersion and aggregation of the θ-Al_2O_3 suspension. Coating of boehmite sol on the θ-Al_2O_3 powders is therefore more favorable at pH conditions (to be more specific, at acidic pH values) to which the powdered suspension is well dispersed.

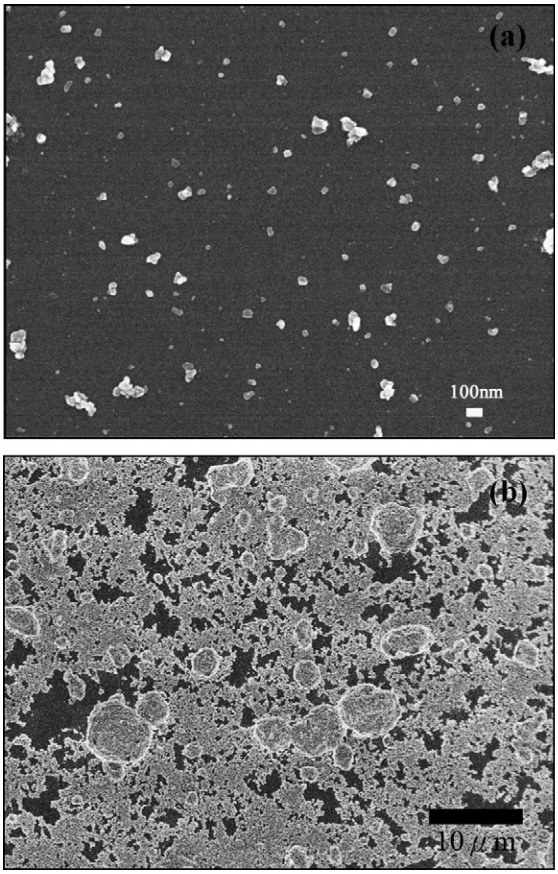

Fig. 2. Particle morphology of dried θ-Al_2O_3 powders prepared at (a) pH 3 and (b) pH 9.

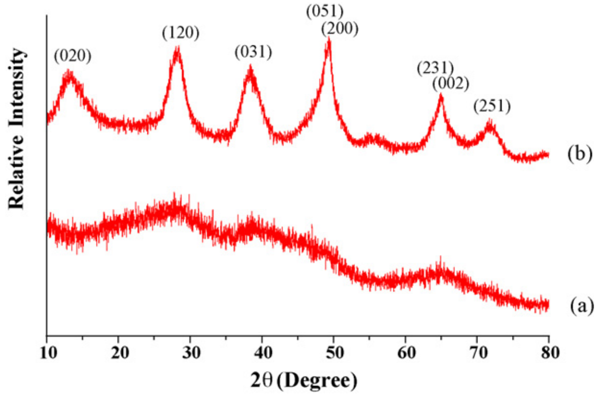

Fig. 3. X-ray diffraction (XRD) patterns of (a) the dried $Al(OC_4H_9)_3$ precursor and (b) the dried boehmite precipitates from the hydrolysis of $Al(OC_4H_9)_3$ precursor in acid at 90 °C.

3.2. Synthesis of boehmite nanoparticles from $Al(OC_4H_9)_3$ precursor

The dried $Al(OC_4H_9)_3$ precursor was amorphous in structure (Fig. 3(a)) from XRD examinations. Hydrolysis of the $Al(OC_4H_9)_3$ precursor in acidic water occurred at a reaction temperature of 90 °C, giving rise to precipitated whitish powder suspended in the solution. The dried, precipitated powder was confirmed the boehmite phase (JCPDS 21-1307) in Fig. 3(b). Particle size determined from the light-scattering technique further revealed a uni-modal size distribution with a narrow particle-size distribution and a mean particle size of 68 nm (Fig. 4). More than 80% of the synthesized particles were found to fall within the size range from 60 to 80 nm. A TEM observation indicates that the boehmite nanoparticles were

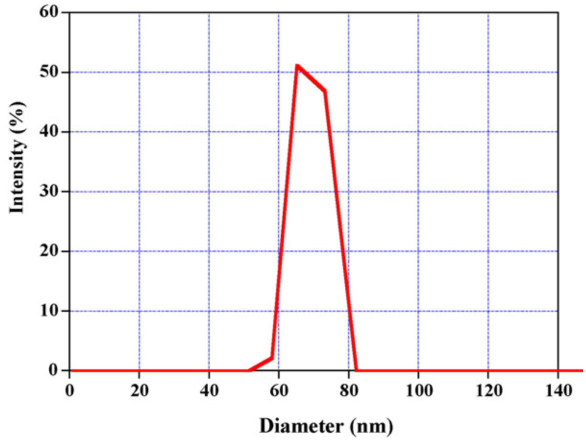

Fig. 4. Particle-size distribution of boehmite nanoparticles determined from the light-scattering technique. The nanoparticles were synthesized from the $Al(OC_4H_9)_3$ precursor in acid at 90 °C.

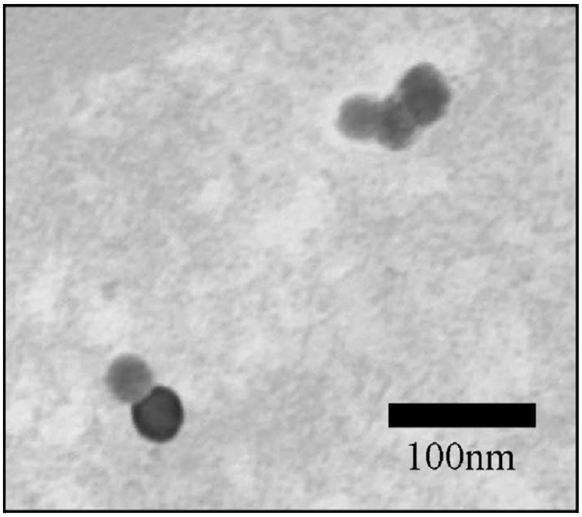

Fig. 5. TEM image of boehmite nanoparticles synthesized from the $Al(OC_4H_9)_3$ precursor in acid at 90 °C.

about spherical in shape (Fig. 5) and tended to form aggregated clusters with an apparent "particle" size in a range similar to that determined by the light-scattering method. The "true" particle size of boehmite may be in the 30 nm range, even though the TEM characterization is arguably sampled in a quantity substantially fewer than that of the light-scattering method.

The formation of boehmite from the hydrolysis of $Al(OC_4H_9)_3$ in acid may be described as follows [14]:

$$Al(OC_4H_9)_{3(l)} + (n+2)H_2O_{(l)} + HCl_{(aq)} \rightarrow AlO(OH)\cdot H_2O_{(s)} + 3C_4H_9OH_{(g)}$$

Nguefack et al. [14] have reported that the $Al(OC_4H_9)_3$ is easily hydrolyzed with excess water because the water molecule is more nucleophilic than the alkoxyl group. Consequently, coordinated water molecules are formed by the nucleophilic reaction from the water molecules and the aluminum atoms in precursor. Lost of protons follows the nucleophilic reaction to form $AlO(OH)\cdot H_2O$ precipitates due to the weakening of oxyhydrogen bonding. On the other hand, the alkoxyl group obtained protons to form alcohol owing to its increasing negative electron affinity. In our experiment, the hydrolysis reaction in acid was markedly expedited by the reaction temperature (90 °C) employed, giving rise to the formation of whitish boehmite nanoparticles in a reduced time. The reaction appeared to complete after an isothermal holding of 30 min from visual inspections.

3.3. Coating of Boehmite nanoparticles on θ-Al_2O_3 particle surface

Fig. 6 shows the infrared absorption spectra of the boehmite/θ-Al_2O_3 mixtures with nominally 3 and 9 wt.% of boehmite concentration after calcination at 600 °C. Absorption peaks exist at 545 and 820 cm^{-1}, respectively, which characterizes the "bare" θ-Al_2O_3 powder (i.e., the as-received θ-Al_2O_3 without the coating treatment). For the boehmite/θ-Al_2O_3 powdered mixtures, the peaks belonging to the θ-Al_2O_3 are no longer apparent; instead, there exist two broad absorption peaks over a wavenumber range from ~500 to 900 cm^{-1}. Shek et al. [15] have reported that these peaks are of the characteristic peaks of γ-Al_2O_3, revealing that the boehmite nanoparticles precipitated from the $Al(OC_4H_9)_3$ precursor favor to coat on the θ-Al_2O_3 particle surface and the coated boehmite "layers" modify the original θ-Al_2O_3 surface. The boehmite coating appeared to transform into γ-Al_2O_3 as temperature was raised to 600 °C. It may be interesting to note that in the boehmite-coating preparation, the $Al(OC_4H_9)_3$ precursor and θ-Al_2O_3 powder were first uniformly mixed in acid solution at pH ~ 3–4 and at temperature of 90 °C. Hydrolysis of the $Al(OC_4H_9)_3$ precursor took place in the solution and then produced OH group on the $AlO(OH)\cdot H_2O$ surface that favored to react with the OH group and the M–OH group of the θ-Al_2O_3 surface by hydrogen adsorption and/or formation of hydrogen bonding at the interface. One might hence suspect that the affinity between the OH groups of the aluminum hydro-oxide and of the θ-Al_2O_3 facilitates the boehmite coating. In addition, the IR absorbance peaks of the boehmite/θ-Al_2O_3 mixtures with 3 and 9 wt.% of boehmite concentration appear virtually identical. This finding suggests that the coating may have reached a saturation at 3 wt.% of boehmite concentration, presumably due to the complete "monolayer" coating of boehmite particles on the available "free" θ-Al_2O_3 surface.

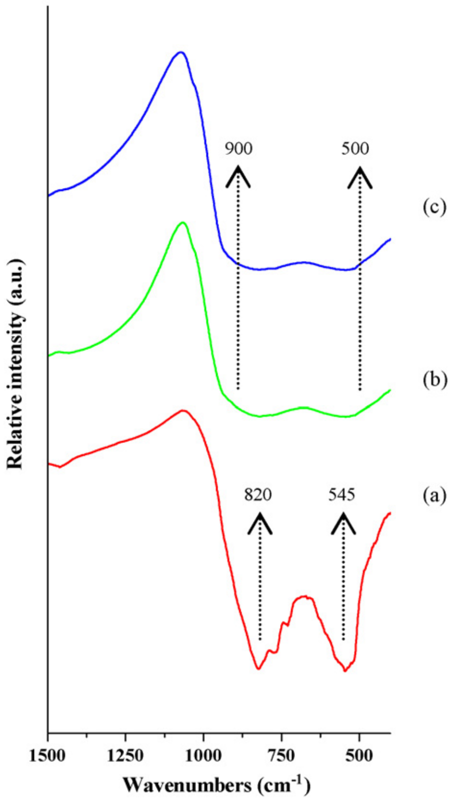

Fig. 6. FTIR absorption spectra of (a) as-received θ-Al_2O_3 powders, (b) 3 wt.% boehmite-coated θ-Al_2O_3 powders and (c) 9 wt.% boehmite-coated θ-Al_2O_3 powder in transmissivity mode. All samples were calcined at 600 °C.

Table 1
Average particle size of θ-Al_2O_3 powders determined from the light-scattering method before and after the coating of boehmite

Boehmite/θ-Al_2O_3 (wt.%)	Average particle size (nm)	
	pH 3	pH 4
0	127 ± 3.72	145 ± 3.80
3	156 ± 1.99	162 ± 2.57
9	150 ± 1.84	160 ± 2.41

Table 1 shows the particle size of calcined θ-Al_2O_3 powder before and after being coated with the boehmite. The average particle size of θ-Al_2O_3 powder appears to increase after the coating for both pH 3 and 4 situations. Consistent with that of the IR results, the particle size did not vary much as the boehmite concentration was increased from 3 to 9 wt.%. The increase in particle size was ∼15–40 nm for the pH examined. This minor increase yet surprised us, since the precipitation of boehmite particles *alone* from the hydrolysis of $Al(OC_4H_9)_3$ precursor (i.e., without the addition of θ-Al_2O_3 powder) has already yielded boehmite nanoparticles with a mean particle size ca. 68 nm. Therefore, the particle-size increase determined from the light-scattering technique appears to be too few for a ‘‘monolayer’’ boehmite-particle coating. Exact reason for this is not known at present. TEM examination of the calcined powders with and without the precursor may throw some light toward the underlying reasons. As shown in Fig. 5, primary particle size of the precipitated boehmite nanoparticles is typically in a size range of ca. 30 nm, while the typical agglomerate size appears comparable to that from the light-scattering method (Fig. 4). Similarly, aggregation of the bare θ-Al_2O_3 particles at solution pH examined also occurs (Fig. 7(a)), forming particle clusters with an irregular shape and with a substantially larger agglomerate size. Therefore, the measured ‘‘particle’’ size in Table 1 is indeed the agglomerate size, making a direct comparison to verify the coating uniformity a difficult task to do.

For the θ-Al_2O_3 powders with 3 wt.% boehmite concentration, the boehmite nanoparticles with a lighter contrast apparently surround the θ-Al_2O_3 powders with a darker contrast in Fig. 7(b). The figure also reveals some coating discontinuities around the θ-Al_2O_3 powders. When the boehmite concentration was increased to 9 wt.%, the agglomeration of boehmite/θ-Al_2O_3 mixtures becomes pronounced even though the coating discontinuity appears less apparent comparatively. A selective area diffraction (SAD) reveals a ring pattern characterizing the polycrystalline nature of the boehmite/θ-Al_2O_3 agglomerates without preferred crystallographic orientations, in contrast to the superposition of ring and spot patterns shown in Fig. 7(c) for the 3 wt.% boehmite case. This finding further indicates possible particle agglomeration induced by the boehmite nanoparticles as the boehmite concentration is increased beyond a critical value.

3.4. Sintered microstructrure

Sintered microstructure of the bare θ-Al_2O_3 powder and the boehmite-coated θ-Al_2O_3 powders is shown in Fig. 8. All the

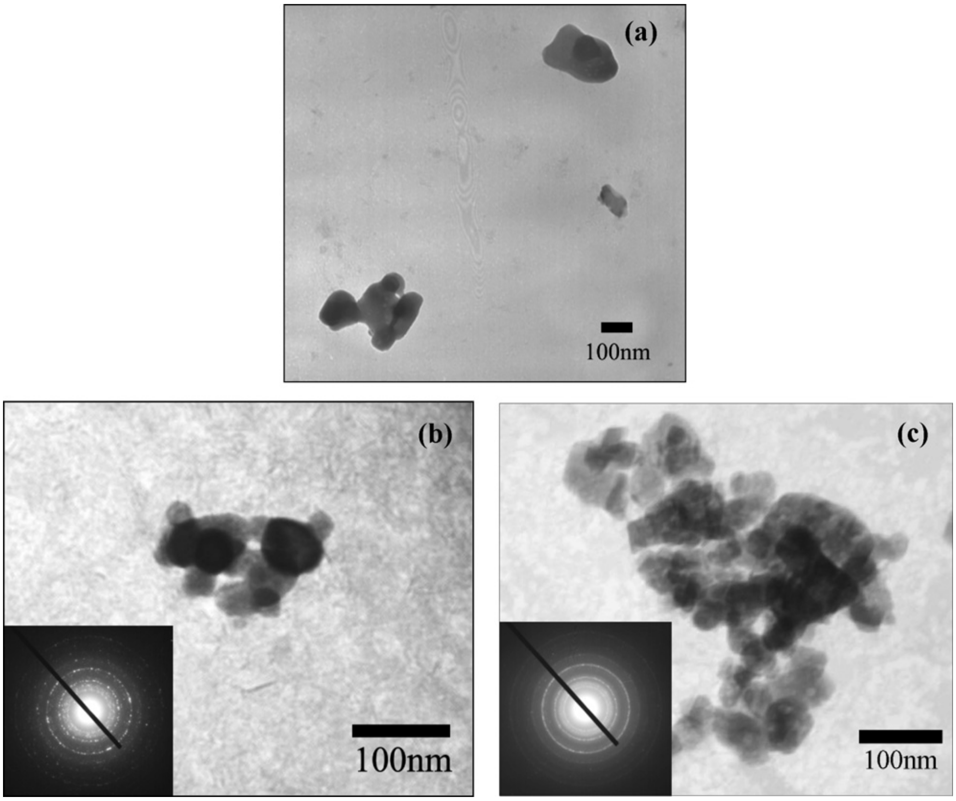

Fig. 7. TEM images of (a) uncoated, bare θ-Al_2O_3 particles dispersed in acid (pH 3–4), and boehmite/θ-Al_2O_3 mixtures with (b) 3 wt.% and (c) 9 wt.% boehmite concentration.

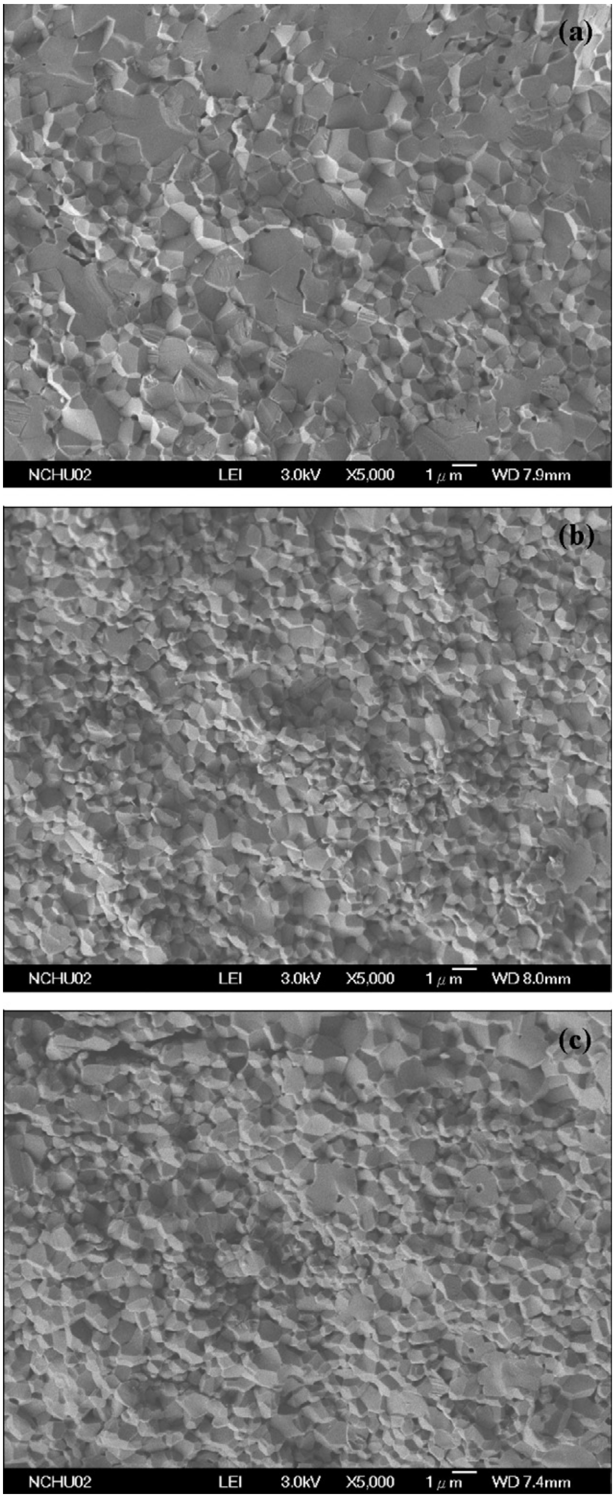

Fig. 8. Fracture surface of (a) bare θ-Al_2O_3 powders, (b) 3 wt.% boehmite-coated θ-Al_2O_3 powders and (c) 9 wt.% boehmite-coated θ-Al_2O_3 powders after sintering at 1500 °C for 2 h.

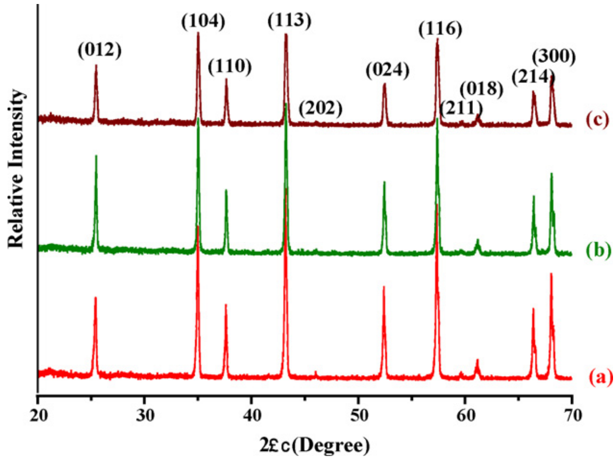

Fig. 9. X-ray diffraction (XRD) patterns of sintered (a) bare θ-Al_2O_3 powders, (b) 3 wt.% boehmite-coated θ-Al_2O_3 powders and (c) 9 wt.% boehmite-coated θ-Al_2O_3 powders. The XRD patterns reveal that all the sintered crystalline phases are of the α-Al_2O_3 phase (JCPDS 46-1212).

samples have a sintered, relative density greater than 90% of the theoretical. A direct comparison from the fractured surfaces reveals that abnormal grain growth becomes more pronounced for the bare θ-Al_2O_3 case (Fig. 8(a)); while, the boehmite-coated ones present a more uniform grain-size distribution (Fig. 8(b and c)). Their crystalline phases were all confirmed the α-Al_2O_3 phase (Fig. 9). This hence suggests that the boehmite coating forms a ‘‘barrier layer’’ which restrains the inter-grain atomic diffusion of the Al_2O_3 matrix so that the abnormal grain growth is inhibited. In addition, the 3 wt.% boehmite-coated Al_2O_3 sample appears to provide the most uniform grain-size distribution, rather than that of the 9 wt.% counterpart. We suspect that the apparent agglomeration of the θ-Al_2O_3 particles (Fig. 7(c)) facilitates the observed grain coarsening upon the isothermal holding.

4. Conclusions

The dispersion property of θ-Al_2O_3 powder suspension can be tailored by pH adjustment; to which, the θ-Al_2O_3 suspension is better dispersed at acidic pH (pH ~ 3–4). The well-dispersed θ-Al_2O_3 particles can be coated with boehmite nanoparticles derived from the hydrolysis of $Al(OC_4H_9)_3$ precursor at a moderate temperature of 90 °C in acidic condition. IR examination confirmed the successful coating of boehmite on θ-Al_2O_3, revealing a formation of γ-Al_2O_3 phase after the samples were calcined at 600 °C in air. It was suspected that the OH groups existing on the aluminum hydro-oxide reacted with the M-OH groups of θ-Al_2O_3 surface favorably due to hydrogen absorption and/or chemical bonding at the interface, hence facilitated the boehmite coating. The agglomerate size determined from the light-scattering method indicated a substantial increase in size after the coating. The coating yet seemed to have reached a saturation as the boehmite concentration exceeds 3 wt.%. TEM examination further reveals that the saturation may indeed arise from the aggregation of boehmite/θ-Al_2O_3 mixtures as the boehmite concentration exceeds the critical concentration. The boehmite coating on θ-Al_2O_3 particle surface has a significant effect on the sintered microstructure. The coating layer acts as a barrier that impedes abnormal grain growth during the θ- to α-phase transformation, resulting in a reduced mean grain size and grain-size distribution.

Acknowledgments

This work was financially supported by the Ministry of Economic Affairs (Taiwan) through contract 92-EC-17-A-08-S1-023. W.J.T. gratefully thanks partial financial support from the National Science Council (Taiwan) under contract NSC 92-2216-E-005-020, and from the Advanced Green Energy Material Project (NCHU) funded by Ministry of Education.

References

[1] H.L. Wen, Y.Y. Chen, F.S. Yen, C.Y. Huang, Size characterization of θ- and α-Al_2O_3 crystallites during phase transformation, Nanostruct. Mater. 11 (1) (1999) 89–101.

[2] H.L. Wen, F.S. Yen, Growth characteristics of boehmite-derived ultrafine theta and alpha-alumina particles during phase transformation, J. Cryst. Growth 208 (2000) 696–708.

[3] J.L. McArdle, G.L. Messing, Seeding with γ-alumina for transformation and microstructure control in boehmite-derived α-alumina, J. Am. Ceram. Soc. 69 (1986) C98–C101.

[4] P.A. Badkar, J.E. Bailey, The mechanism of simultaneous sintering and phase transformation in alumina, J. Mater. Sci. 11 (1976) 1794–1806.

[5] K.R. Han, C.S. Lim, M.J. Hong, Preparation method of submicrometer-size α-alumina by surface modification of γ-alumina with alumina sol, J. Am. Ceram. Soc. 83 (4) (2000) 750–754.

[6] Q. Yang, T. Troczynski, Dispersion of alumina and silicon carbide powers in alumina sol, J. Am. Ceram. Soc. 82 (7) (1999) 1928–1930.

[7] S. Ananthakumar, V. Raja, K.G.K. Warrier, Effect of nanoparticulate boehmite sol as a dispersant for slurry compaction of alumina ceramics, Mater. Lett. 43 (2000) 174–179.

[8] W.H. Shih, L.L. Pwu, A.A. Tseng, Boehmite coating as consolidation and forming aid in aqueous silicon nitride processing, J. Am. Ceram. Soc. 78 (5) (1995) 1252–1260.

[9] C.Y. Yang, W.H. Shih, Effect of acid on the coating of boehmite onto silicon carbide particles in aqueous suspensions, J. Am. Ceram. Soc. 82 (2) (1999) 436–440.

[10] C.Y. Yang, W.Y. Shih, W.H. Shih, Effects of boehmite-coating thickness on the consolidation and rheological properties of boehmite-coating SiC suspensions, J. Am. Ceram. Soc. 84 (12) (2001) 2834–2840.

[11] H.J. Youn, J.W. Jang, I.T. Kim, K.S. Hong, Low-temperature formation of α-alumina by doping of an alumina-sol, J. Colloid Interface Sci. 211 (1999) 110–113.

[12] C.Y. Yang, W.Y. Shih, W.H. Shih, Gelation, consolidation, and rheological properties of boehmite-coated silicon carbide suspension, J. Am. Ceram. Soc. 83 (8) (2000) 1879–1884.

[13] J.S. Reed, Principles of Ceramics Processing, John Wiley and Sons, New York, 1995, pp. 162–168.

[14] M. Nguefack, A.F. Popa, S. Rossignol, C. Kappenstein, Preparation of alumina through a sol-gel process. Synthesis, characterization, thermal evolution and model of intermediate boehmite, Phys. Chem. Chem. Phys. 5 (2003) 4279–4289.

[15] C.H. Shek, J.K.L. Lai, T.S. Gu, G.M. Lin, Transformation evolution and infrared absorption spectra of amorphous and crystalline nano-Al_2O_3 powders, NanoStruct. Mater. 8 (5) (1997) 605–610.